Magnetic Structure of αTb2C3

Masao Atoji

Citation: The Journal of Chemical Physics **54**, 3504 (1971); doi: 10.1063/1.1675373
View online: http://dx.doi.org/10.1063/1.1675373
View Table of Contents: http://scitation.aip.org/content/aip/journal/jcp/54/8?ver=pdfcov
Published by the AIP Publishing

Magnetic Structure of α-Tb_2C_3*

MASAO ATOJI
Chemistry Division, Argonne National Laboratory, Argonne, Illinois 60439

(Received 24 September 1970)

Neutron powder diffraction measurements have shown that, in the body-centered cubic α-Tb_2C_3 below 33 ± 4°K, two out of four body-diagonally linked Tb arrays become antiferromagnetic linear chains but the two remaining Tb arrays exhibit no ordered moment. The nearest Tb atoms between the different ordered spin arrays are related ferromagnetically. Six alternative ways of choosing two body-diagonal antiferromagnetic arrays are mutually equivalent due to the crystal symmetry but not to the multiplet degeneracy in powder diffractometry. The moments are most likely directed along the face diagonal which lies in the plane formed by two body diagonals parallel to the ordered spin arrays. The next probable moment direction lies longitudinally along any one of the two ordered arrays. The saturation moment per magnetically ordered Tb in these collinear spin structures is very insensitive to the selection of the moment direction and approximates closely the free Tb^{3+} value of 9 μ_B. An equivalent multiaxial antiferrostructure is obtained by combining two collinear magnetic structures with the mutually orthogonal face-diagonal moments. In this alternative biaxial structure, all Tb atoms possess the same saturation ordered moment of $9/\sqrt{2}$ μ_B. A sizeable magnetic diffuse scattering having the modulation of an apparently ferromagnetic short-range order was observed in the magnetically long-range ordered region.

INTRODUCTION

The rare earth sesquicarbides, represented by $(RE)_2C_3$ with a nonstoichiometric allowance of up to several atomic percent, are classified into two major structural categories, the body-centered cubic α-Pu_2C_3 type[1] (RE=La, Ce, Pr, Nd, Sm, Gd, Tb, Dy, and Ho)[2] and the noncubic $\delta-Y_2C_3$ type[3] (RE=Er, Tm, and Lu).[2] Stoichiometric Yb_2C_3, however, does not exist and $YbC_{1.25-1.4}$ exhibits a monoclinic symmetry.[4] Further, the reported result together with our findings indicates that $(RE)_2C_3$ with RE=Tb, Dy, and Ho prepared by the standard annealing technique frequently contain the δ-Y_2C_3-type second phase.[2] Y_2C_3 forms the α-Pu_2C_3-type structure under high pressure.[5] The actinide-series counterparts of the light RE, U_2C_3 [6] and Np_2C_3,[7] are also isostructural with α-Pu_2C_3. The *d*-shell transition metals are not known to form the stable higher carbides such as the sesquicarbide and the dicarbide, but further preparatory investigation is desirable in this area. Among the different structures found in the sesquicarbide category, only the α-Pu_2C_3-type structure has been completely determined,[8,9] and its magnetic structure is the subject of this study.

α-$(RE)_2C_3$ is golden metallic. The electrical resistivity of α-La_2C_3 at room temperature[2] is 144×10^{-6} $\Omega\cdot$cm which is comparative to that of the La metal, 57×10^{-6} $\Omega\cdot$cm.[10] This pure metallike conductivity of $(RE)_2C_3$ should facilitate the RKKY-type exchange coupling among 4*f* electrons and consequently the magnetic ordering at accessibly low temperatures. The paramagnetic neutron scattering data of α-$(RE)_2C_3$ with RE=Pr and Tb at room temperature[9] are representative of the free tripositive rare earth ion in the Hund ground state. Singularly, the effective valency of Ce in α-Ce_2C_3 is +3.4 at room temperature, corresponding to a statistical population of 0.6 unpaired electrons per Ce in the 4*f* band.[9] In cooling α-Ce_2C_3, an electronic transition of the 4*f*-to-valency band takes place gradually, leaving an empty 4*f* band at temperatures below 80°K. As a consequence, no magnetic ordering was observed in α-Ce_2C_3 at temperatures down to 2°K.[11] No other reliable data have been reported on the physical properties of $(RE)_2C_3$ at low temperatures. In contrast, the magnetic susceptibility, the electrical resistivity, and the thermoelectric power of α-U_2C_3 and those of α-Pu_2C_3 have been measured, revealing the onset of magnetic ordering at 50 and 120°K, respectively.[12,13] A neutron powder diffraction study of α-U_2C_3 was, however, unable to determine the ordered spin structure owing to the small ordered moment of less than about 0.8 μ_B.[5]

The carbon atoms in the α-Pu_2C_3-type structure are dimerized to form the C_2 molecular group which is markedly stabilized in the C_2^{2-} state.[8] The valence electron orbitals of the C_2^{2-} group are considerably aspherical, enhancing the crystal field anisotropy and also the *d*-orbit contribution of the metal atom in the conduction band formation.[14] A rich variety of experimental manifestations of the anisotropic 5*d*–4*f* RKKY interaction are amply demonstrated by the ordered magnetic structures of the centrosymmetric REC_2.[14,15] On the other hand, the α-Pu_2C_3-type structure is highly asymmetric, and hence the RKKY interaction and the crystal-field effect should reflect this uniqueness. It is hoped that the magnetic structure of α-Tb_2C_3 described hereafter and that of α-Ho_2C_3 in the following paper enrich our knowledge in these specific aspects. The experimental uncertainty in this paper is given in terms of standard deviation.

CRYSTALLOGRAPHIC DATA

As depicted in the phase diagrams of the La–C,[16] Y–C,[3] Yb–C,[4] and U–C [17] systems, $(RE)_2C_3$ and its homologues melt incongruently. Moreover, the second-phase contamination is almost inevitable in the routine preparatory technique. Hence, no attempt was made to

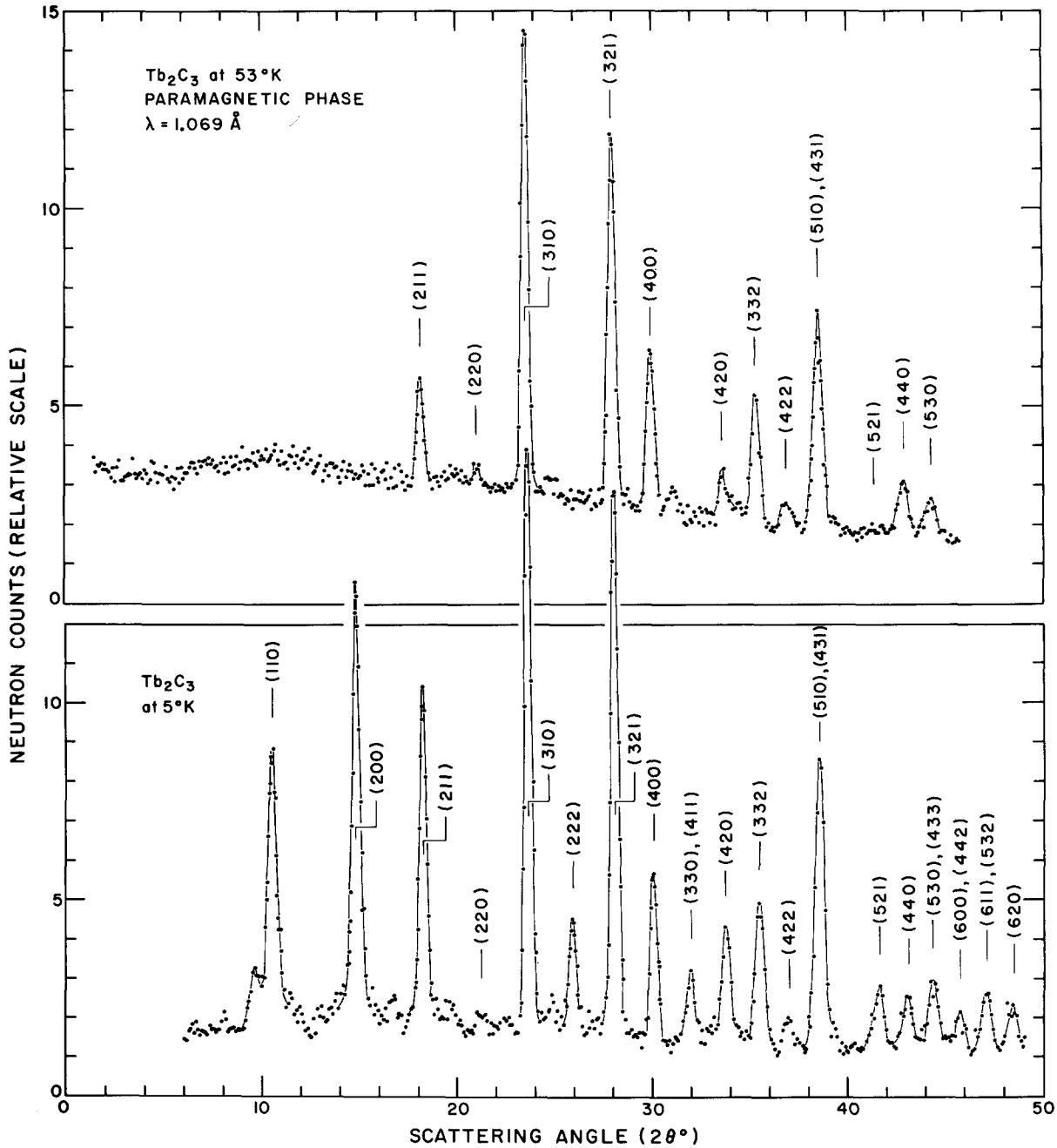

FIG. 1. Neutron diffraction patterns of α-Tb_2C_3. The nuclear and magnetic indices of α-Tb_2C_3 are given in the 53 and 5°K patterns, respectively. Relatively weak, unindexed peaks in the 53°K pattern are the nuclear reflections of TbC_2 and those of δ-Tb_2C_3. In the 5°K pattern, the total scattering intensities of TbC_2 (the coherent reflections and the diffuse scattering of both nuclear and magnetic origins) have been subtracted, leaving the nuclear and magnetic reflections of α-Tb_2C_3 and the weak unindexed nuclear and magnetic peaks of δ-Tb_2C_3.

grow single crystals of $(RE)_2C_3$. Polycrystalline α-Tb_2C_3 was prepared by arc melting the compressed pellets composed of the stoichiometric amounts of Tb metal filings (99.9% pure) and spectroscopic-grade graphite powders.[2] $(RE)_2C_3$ is susceptible to hydrolytic decomposition, and therefore, the sample handling was always carried out in helium atmosphere. The arc-melted buttons were pulverized and packed into the null-matrix Ti–Zr holder. Neutron diffraction patterns were taken using the multipurpose diffractometer with the wavelength set for $\lambda = 1.069$ Å. Extraneous nuclear reflections were identified as due to 11.0 ± 0.4 wt% of

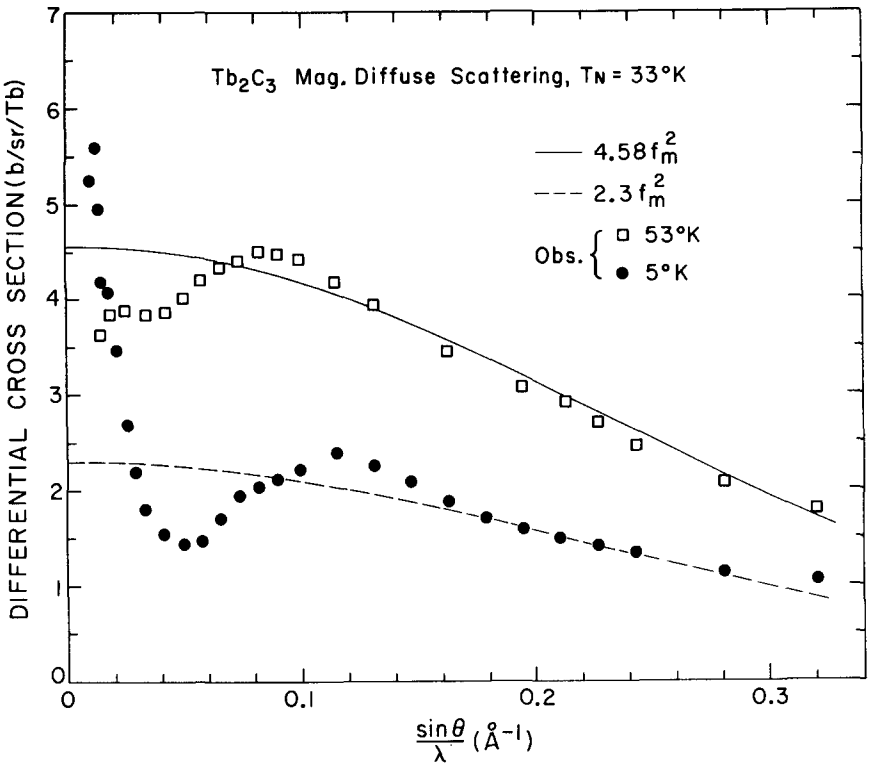

FIG. 2. Magnetic diffuse scattering of α-Tb_2C_3 including the δ-Tb_2C_3 contribution of doubtful significance. The solid curve represents the paramagnetic differential cross section of the free Tb^{3+} ion (the Trammell magnetic form factor f_m with $Z-S=22$) which approximate closely the observed value of α-Tb_2C_3 at room temperature. The dotted curve is the median curve of the diffuse scattering at 5°K.

TbC_2 and to approximately several percent of δ-Tb_2C_3. No other impurities were detectable in the neutron and x-ray diffraction inspections. The neutron diffraction data of TbC_2 at temperatures down to 2°K are available[14] and were subtracted from the Tb_2C_3 patterns. The d spacings of δ-Tb_2C_3 were found to be similar to the x-ray d-spacing values of δ-Y_2C_3.[3] Although the crystal structure of δ-$(RE)_2C_3$ is unknown, several intense, isolated nuclear reflections are not contaminated by the impurity reflections and were used for obtaining the absolute intensities of the magnetic reflections.

The cubic lattice constants are $a=8.2526$, 8.2400, and 8.2375 Å (± 0.0006 Å for all values) at 296, 79, and 5°K, respectively. The average linear thermal expansion coefficient in the range 5–296°K is hence 6.3 ± 0.4 in 10^{-6} deg^{-1} which is comparable to those of REC_2 [14] and hence is not indicative of unusual magnetostriction. The positional parameters in $T_d^6-I\,\bar{4}3d$ have previously been determined as Tb at 16(c) (u, u, u) with $u=0.0516\pm 0.0004$ and C at 24(d) $(v, 0, 1/4)$ with $v=0.2999\pm 0.0003$.[9] The Debye–Waller temperature factors are $2B=2.9\pm 0.4$ Å^2 at 296°K and 0.4 ± 0.1 A^2 at 5°K. The diffraction pattern at 53 and the one at 5°K are shown in Fig. 1.

MAGNETIC STRUCTURE

In cooling below room temperature, a wavy modulation of the paramagnetic scattering becomes enhanced. This modulation is quite analogous to the TbC_2 case[14] and is readily interpretable as due to the effectively antiferromagnetic near-neighbor spin couplings (Fig. 2). At 33 ± 4°K, a set of additional reflections starts to grow at the expense of paramagnetic scattering and therefore are assumed to be originated from the magnetic long-range ordering. The observed magnetic reflections were all indexable on the basis of the chemical unit-cell dimensions (Fig. 1). The temperature-dependency data of the magnetic reflections of α-Tb_2C_3 suffer from relatively large experimental errors. Nevertheless, it is certain that the spontaneous magnetization reaches essentially the saturation value near 5°K. All of the weak unindexable magnetic reflections could be assigned as due to δ-Tb_2C_3. The magnetic unit-cell volume of δ-Tb_2C_3 is at least twice as large as the chemical unit-cell volume and the onset of the magnetic ordering takes place around 30 ± 5°K.

In analyzing the magnetic structure of α-Tb_2C_3, the atomic coordinates[18] are conveniently rearranged as follows: $(0, 0, 0)$; $(\frac{1}{2}, \frac{1}{2}, \frac{1}{2},)+$

(1), u, u, u;	(5), $\frac{1}{4}+u, \frac{1}{4}+u, \frac{1}{4}+u$;
(2), $u, -u, \frac{1}{2}-u$;	(6), $\frac{1}{4}+u, \frac{3}{4}-u, \frac{1}{4}-u$;
(3), $\frac{1}{2}-u, u, -u$;	(7), $\frac{1}{4}-u, \frac{1}{4}+u, \frac{3}{4}-u$;
(4), $-u, \frac{1}{2}-u, u$;	(8), $\frac{3}{4}-u, \frac{1}{4}-u, \frac{1}{4}+u$.

We write (1′), (2′), (3′), etc., for the coordinates generated by the body-centering translation (Fig. 3). The

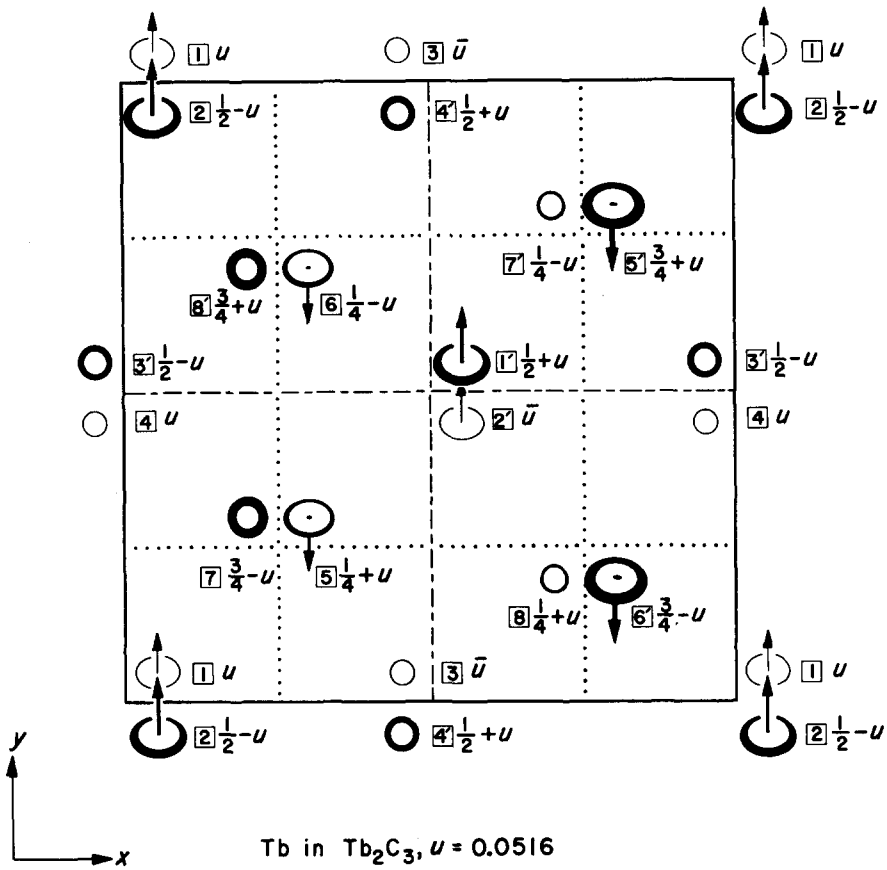

FIG. 3. The most probable uniaxial ordered magnetic structure of α-Tb_2C_3 projected on the xy plane. The ordered antiferromagnetic arrays are chosen parallel to the [111] and [$\bar{1}$11] axes, for which the most likely spin direction is parallel to the [011] axis as shown here. The z-axis coordinates of the Tb sites are also given. The carbon atoms are not shown.

sites (1)–(4) generate (5)–(8), respectively, through the diamond-glide operation.

The indices of the observed magnetic reflections satisfy the body-centering condition, $h+k+l=2n$, implying the spins at (1), (2), (3), etc., are parallel to those at (1′), (2′), (3′), etc., respectively. In addition, the magnetic reflections having the diamond-glide condition, $h+k+l=4n$ with h and k (and l) being all even, are unobservably weak or attributable to δ-Tb_2C_3. This means that the spins at (1)–(4) are antiparallel to those at (5)–(8), respectively. Consequently, the problem is to find the spin directions and magnitudes at (1)–(4). The observed intensities are not at all compatible with any of the conceivable models in which different or equal spins are assigned to all sites. A satisfactory result was obtained when one assumes the same spin at any two sites amongst (1)–(4) and no ordered spin at the remaining two sites. For instance, when one assigns the (+) spins to (1), (2), (1′), and (2′), we have the (−) spins at (5), (6), (5′), and (6′) but no ordered spin at the other sites.

The resultant magnetic structure is conveniently described as follows: There are four kinds of linear chains of the Tb atoms in α-Tb_2C_3, that is, (1)–(5)–(1′)–(5′), (2)–(6′)–(2′)–(6), (3)–(7′)–(3′)–(7), and (4)–(8′)–(4′)–(8), which are parallel to the [111], [$\bar{1}$11], [1$\bar{1}$1], and [11$\bar{1}$] axes, respectively. The neighboring interatomic distance along these body diagonals is given representatively by (1)–(5) = (1)–(5′) = 3.566±0.001 Å at 5°K, which is the second shortest Tb–Tb approach in α-Tb_2C_3. We abbreviate for instance the (1)–(5)–(1′)–(5′) array as the (1) linear chain. Any two out of these four linear chains exhibit individually an antiferromagnetic moment array, and the remaining two linear chains have no ordered moment. The shortest Tb–Tb approaches in the structure, (1)–(2) = (1)–(3) = (1)–(4) = 3.377±0.005 Å at 5°K, are interconnecting between the different body-diagonal Tb arrays and are ferromagnetically correlated in the ordering scheme. Consequently, as far as the black-and-white spin configuration is concerned, there are six different choices in placing the spins on two selected body-diagonal linear chains. However, all six choices are mutually equivalent and are related through the permutable exchanges of the cube axes with or without the invariant translation of the origin of the chemical unit cell. A single crystal study would lead to the same conclusion. It should be emphasized that the magnetic structure of α-Tb_2C_3 is no longer cubic but possesses a noncentrosymmetric orthorhombic symmetry.

The ambiguity associated with the multiplet characteristics of the powder reflection arises in the determina-

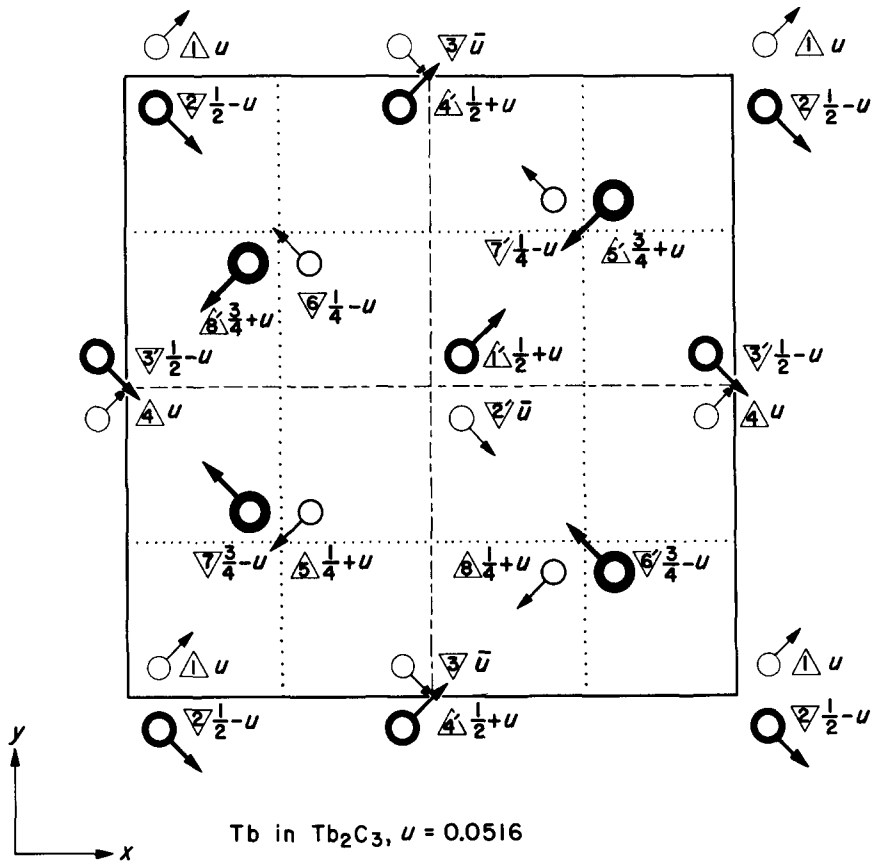

FIG. 4. An exemplary biaxial magnetic structure of α-Tb_2C_3 obtained by combining two different uniaxial structures with the mutually perpendicular moment directions. The Tb atoms designated by

etc., belong to the first uniaxial magnetic structure and those with

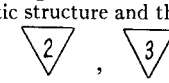

etc., belong to the second uniaxial structure.

tion of the moment direction. Let us assume that the moment direction is parallel (or antiparallel) to the crystals axis $[hkl]$. When we place the ordered moments at the (1) and (2) linear chains, for instance, the powder diffraction data cannot distinguish among the moment directions, $[hkl]$, $[\bar{h}kl]$, $[h\bar{k}l]$, and $[\bar{h}\bar{k}l]$. More specifically, for the principal axial directions, this directional ambiguity may be written as $[100]\neq[010]=[001]$, $[110]=[101]=[\bar{1}10]=[\bar{1}01]\neq[011]\neq[01\bar{1}]$, $[111]=[\bar{1}11]\neq[1\bar{1}1]$, and $[1\bar{1}1]=[11\bar{1}]$. The calculated intensities for these seven distinguishable, specific directions were compared with the observed intensities at 5°K (Table I). The resultant discrepancy factor, $R=\Sigma\,|\,I_{\rm obs}-I_{\rm calc}\,|/\Sigma I_{\rm obs}$, are 9.3%, 13%, 17%, 22%, 28%, 31%, and larger than 31% for the moment directions parallel to [011], [111], [001], [110], $[1\bar{1}1]$, [100], and $[01\bar{1}]$, respectively. In view of these over-all R factors and the agreement with respect to several especially reliable $I_{\rm obs}$'s, the moment directions are most likely parallel to [011] and slightly less likely parallel to [111] or $[\bar{1}11]$. In other words, the most probable moment direction is parallel to the face diagonal which lies in the plane formed by the two body-diagonals parallel to the ordered linear chains. The next probable moment direction is parallel to either one of the ordered spin arrays.

The ordered moment value gJ is highly insensitive to the choice of the moment direction and the saturation values lie in the range from 8.8 to 9.0 μ_B. The [011] and [111] moment directions give $gJ=8.84\pm0.18$ and 8.87 ± 0.26 μ_B, respectively, both of which are slightly but insignificantly smaller than the free Tb^{3+} value of 9 μ_B. The Trammell magnetic form factor with $Z-S=22$ [19] (Fig. 2) was employed in $I_{\rm calc}$ (Table I). The most probable collinear spin structure of α-Tb_2C_3 is illustrated in Fig. 3.

We have so far discussed the collinear or uniaxial magnetic structure. We may superimpose two different uniaxial magnetic structures, provided that their collinear moment directions are mutually orthogonal within a given coherent domain. For example, firstly we place the ordered spins on the (1) and (4) linear chains for which the most probable moment direction is parallel to [110]. We then choose the ordered spins on the (2) and (3) chains since the most likely moment direction for this second structure is $[\bar{1}10]$ which is perpendicular to [110]. In this biaxial structure, as illustrated in Fig. 4, all atoms are magnetically ordered and the saturation moment value is $8.87/\sqrt{2}=6.27$ μ_B. The biaxial structure with the next likely moment directions (the body-diagonal axes) is illogical because the orthogonality criterion is not satisfied.

As seen in Fig. 2, a sizeable magnetic diffuse scattering was observed in the temperature range where the

spontaneous magnetization has reached to its maximum value. The median curve of the magnetic diffuse scattering at 5°K gives an apparent, disordered magnetic moment of $6.9\pm0.8\ \mu_B$. On the other hand, an anticipated residual disordered magnetic moment may be calculated as

$$\{[g^2J(J+1) \text{ for the free } Tb^{3+}] - \langle (gJ)_{obs}{}^2\rangle_{Av}\}^{1/2}$$
$$= [94.5-(78/2)]^{1/2} = 7.4\mu_B,$$

which is in agreement with the observed value. Both the collinear and biaxial magnetic structures lead to the same result. A predominantly ferromagnetic short-range order among these residual moments gives rise to the wavy modulation of the observed diffuse cross section curve (Fig. 2).[20] No unique interpretation of this short-range order interaction is possible, since the curve fitting analysis indicates a sizeable, cumulative contribution from the second and third Tb–Tb neighbors.

TABLE I. Observed and calculated magnetic intensities in barns per Tb of the collinear spin structures of α-Tb_2C_3. The Tb arrays parallel to [111] and [$\bar{1}$11] are selected as the magnetically ordered linear chains. The calculated values are given for the most likely moment direction [011], the next likely direction [111], and an unlikely direction [001]. The observed values in brackets are highly unreliable owing to a large uncertainty in the peak resolving procedure and hence are excluded in the parameter determination.

Indices	I_{obs}	I_{calc} [011]	I_{calc} [111]	I_{calc} [001]
110	(375)	478	506	592
200	514	486	454	484
211	244	216	249	215
220	<4	0	0	0
310	(150)	202	194	180
222	145	154	140	107
321	206	259	280	306
400	<4	0	0	0
330	91	30	39	48
411		69	74	71
420	138	124	110	110
332	(72)	40	39	41
422	<4	0	0	0
431	120	80	81	76
510		43	49	50
521	89	90	90	80

* Based on work performed under the auspices of the U.S. Atomic Energy Commission.

[1] W. H. Zachariasen, Acta Cryst. **5,** 17 (1952).
[2] F. H. Spedding, K. Gschneidner, Jr., and A. H. Daane, J. Am. Chem. Soc. **80,** 4499 (1958).
[3] O. N. Carlson and W. M. Paulson, Trans. AIME **242,** 846 (1968).
[4] J. M. Haschke and H. A. Eick, J. Am. Chem. Soc. **92,** 1526 (1970).
[5] M. C. Krupka, A. L. Giorgi, N. H. Krikorian, and E. G. Szklarz, J. Less-Common Metals **17,** 91 (1969).
[6] C. DeNovion, J.-P. Krebs, and P. Mériel, Comp. Rend. Acad. Sci. Paris **B263,** 457 (1966).
[7] R. Lorenzelli, Comp. Rend. Acad. Sci. Paris **C266,** 900 (1968).
[8] M. Atoji, K. Gschneidner, Jr., A. H. Daane, R. E. Rundle, and F. H. Spedding, J. Am. Chem. Soc. **80,** 1804 (1958).
[9] M. Atoji and D. E. Williams, J. Chem. Phys. **35,** 1960 (1961).
[10] K. Gschneidner, Jr., *Rare Earth Alloys* (Van Nostrand, Princeton, N.J., 1961).
[11] M. Atoji, J. Chem. Phys. **46,** 4148 (1967).
[12] P. Costa, R. Lallement, F. Anselin, and D. Rossignal, in *International Symposium on Compounds of Interest in Nuclear Reactor Technology*, edited by J. T. Waber, P. Chiotti, and W. N. Minor (AIME, 1964), pp. 83–91.
[13] C. DeNovion, P. Costa, and G. Dean, Phys. Letters **19,** 455 (1965).
[14] M. Atoji, J. Chem. Phys. **46,** 1891 (1967).
[15] M. Atoji, J. Chem. Phys. **48,** 3384 (1968).
[16] F. H. Spedding, K. Gschneidner, Jr., and A. H. Daane, Trans. AIME **215,** 192 (1959).
[17] W. B. Wilson, J. Am. Ceram. Soc. **43,** 77 (1960).
[18] *International Tables for X-ray Crystallography*, edited by N. F. M. Henry and K. Lonsdale (Kynoch, Birmingham, England, 1952), Vol. 1.
[19] M. Atoji, J. Chem. Phys. **35,** 1950 (1961).
[20] G. T. Trammell, Phys. Rev. **131,** 932 (1963).